Fernley, R. T., Coghlan, J. P., & Wright, R. D. (1988a) *Biochem. J. 249*, 201-207.
Fernley, R. T., Wright, R. D., & Coghlan, J. P. (1988b) *Biochemistry 27*, 2815-2820.
Fernley, R. T., Darling, P., Aldred, P., Wright, R. D., & Coghlan, J. P. (1989) *Biochem. J. 259*, 91-96.
Forsman, C., Behravan, G., Jonsson, B.-H., Liang, Z.-W., Lindskog, S., Ren, X., Sandstrom, J., & Wallgren, K. (1988) *FEBS Lett. 229*, 360-362.
Frohman, M. A., Dush, M. K., & Martin, G. R. (1988) *Proc. Natl. Acad. Sci. U.S.A. 85*, 8998-9002.
Kozak, M. (1987) *Nucleic Acids Res. 15*, 8125-8148.
Kyte, J., & Doolittle, R. F. (1982) *J. Mol. Biol. 157*, 105-132.
Lloyd, J., McMillan, S., Hopkinson, D., & Edwards, Y. (1986) *Gene 41*, 233-239.
Maniatis, T., Fritsch, E. F., & Sambrook, J., (1982) *Molecular Cloning: A Laboratory Manual*, Cold Spring Harbor Laboratory, Cold Spring Harbor, NY.
Montgomery, J. C., Venta, P. J., Tashian, R. E., & Hewett-Emmett, D. (1987) *Nucleic Acids Res. 15*, 4687.
Murakami, H., & Sly, W. S. (1987) *J. Biol. Chem. 262*, 1382-1388.
Notstrand, B., Vaara, I., & Kannan, K. K. (1975) in *Isozymes: Molecular Structure* (Markert, C. L., Ed.) Vol. 1, pp 575-599, Academic Press, New York.
Penschow, J. D., Haralambidis, J., Aldred, P., Tregear, G. W., & Coghlan, J. P. (1986) *Methods Enzymol. 124*, 534-548.
Proudfoot, N. J., & Brownlee, G. G. (1976) *Nature (London) 263*, 211-214.
Saiki, R. K., Gelfand, D. H., Stoffel, S., Scharf, S. J., Higuchi, R., Horn, G. T., Mullis, K. B., & Erlich, H. A. (1988) *Science 239*, 487-491.
Sanger, F., Nicklin, S., & Coulsen, A. R. (1977) *Proc. Natl. Acad. Sci. U.S.A. 74*, 5463-5467.
Southern, E. M. (1975) *J. Mol. Biol. 98*, 503-517.
Staden, R. (1977) *Nucleic Acids Res. 10*, 4731-4751.
Storey, B. T., Dodgson, S. J., & Forster, R. E., II (1984) *Ann. N.Y. Acad. Sci. 429*, 210-211.
Sutherland, G. R., Baker, E., Fernandez, K. E. W., Callen, D. F., Aldred, P., Coghlan, J. P., Wright, R. D., & Fernley, R. T. (1989) *Cytogenet. Cell Genet. 50*, 149-150.
Tashian, R. E. (1989) *BioEssays 10*, 186-192.
Venta, P. J., Montgomery, J. C., Hewett-Emmett, D., Wiebauer, K., & Tashian, R. E. (1985) *J. Biol. Chem. 260*, 12130-12135.
Venta, P. J., Montgomery, J. C., & Tashian, R. E. (1987) *Isozymes: Curr. Top. Biol. Med. Res. 14*, 59-72.
Wade, R., Gunning, P., Eddy, R., Shows, T., & Kedes. L. (1986) *Proc. Natl. Acad. Sci. U.S.A. 83*, 9571-9575.
Wistrand, P. J. (1984) *Ann. N.Y. Acad. Sci. 429*, 195-206.

Solution Structure of Human Calcitonin Gene-Related Peptide by ^{1}H NMR and Distance Geometry with Restrained Molecular Dynamics†

Alexander L. Breeze, Timothy S. Harvey, Renzo Bazzo, and Iain D. Campbell*
Department of Biochemistry, University of Oxford, South Parks Road, Oxford OX1 3QU, U.K.
Received June 5, 1990; Revised Manuscript Received September 11, 1990

ABSTRACT: The structure of human calcitonin gene-related peptide 1 (hCGRP-1) has been determined by ^{1}H NMR in a mixed-solvent system of 50% trifluoroethanol/50% H_2O at pH 3.7 and 27 °C. Complete resonance assignment was achieved by using two-dimensional methods. Distance restraints for structure calculations were obtained by semiquantitative analysis of intra- and interresidue nuclear Overhauser effects; in addition, stereospecific or χ^1 rotamer assignments were obtained for certain side chains. Structures were generated from the distance restraints by distance geometry, followed by refinement using molecular dynamics, and were compared with experimental NH–CαH coupling constants and amide hydrogen exchange data. The structure of hCGRP-1 in this solvent comprises an amino-terminal disulfide-bonded loop (residues 2–7) leading into a well-defined α-helix between residues 8 and 18; thereafter, the structure is predominantly disordered, although there are indications of a preference for a turn-type conformation between residues 19 and 21. Comparison of spectra for the homologous hCGRP-2 with those of hCGRP-1 indicates that the conformations of these two forms are essentially identical.

Calcitonin gene-related peptide (CGRP)[1] is a 37 amino acid residue single-chain polypeptide which is characterized by a carboxy-terminal phenylalanine amide and an amino-terminal disulfide-bonded loop. Two forms of CGRP (designated α- and β-CGRP, or CGRP-1 and CGRP-2) were predicted to arise as alternative splicing products of the α- and β-calcitonin gene complexes (Amara et al., 1982; Rosenfeld et al., 1983; Hoppener et al., 1985; Steenbergh et al., 1985); the existence of CGRP-1 in man was confirmed following its isolation and characterization by fast atom bombardment mass spectrometry (Morris et al., 1984). The peptide was subsequently found to have a widespread distribution in the body, being particularly prevalent in the central nervous system, and peripherally in nerves of the cardiovascular system (Gibson et al., 1984).

† This is a contribution from the Oxford Centre for Molecular Sciences which is supported by the SERC and MRC. A.L.B. and T.S.H. were supported additionally by ICI.
* Address correspondence to this author.

[1] Abbreviations: CGRP, calcitonin gene-related peptide; CD, circular dichroism; NMR, nuclear magnetic resonance; hCGRP, human CGRP; DG, distance geometry; REM, restrained energy minimization; RMD, restrained molecular dynamics; TFE, trifluoroethanol; HOHAHA, homonuclear Hartmann–Hahn spectroscopy; DQF-COSY, double-quantum-filtered two-dimensional correlation spectroscopy; E.COSY, exclusive correlation spectroscopy; NOESY, two-dimensional nuclear Overhauser effect spectroscopy; TPPI, time-proportional phase incrementation; rms, root mean square.

0006-2960/91/0430-575$02.50/0

Apart from its likely role as a neurotransmitter or neuromodulator in spinal cord and other central neurones (Rosenfeld et al., 1983; Fisher et al., 1983; Kimura et al., 1987), there is direct evidence for the involvement of CGRP in the regulation of both peripheral and arterial blood flow; indeed, it is among the most potent vasodilatory substances known (Struthers et al., 1986).

A further facet to the action of CGRP was recently unveiled following the isolation of the major monomer component of pancreatic islet amyloid, deposition of which is characteristic of type 2, or non-insulin-dependent, diabetes mellitus. The molecule, termed amylin, was found to be a polypeptide of 37 residues bearing 46% sequence homology to human CGRP-2 (Westermark et al., 1987; Cooper et al., 1987). Subsequent studies have shown that both amylin and CGRP are potent in vitro inhibitors of basal and insulin-stimulated glycogen synthesis in skeletal muscle (Leighton & Cooper, 1988; Cooper et al., 1988) and have implicated amylin both as a possible factor in the pathophysiology of type 2 diabetes and in the normal regulation of insulin-mediated metabolic processes.

In view of the manifold and potent actions of CGRP, and its structural and functional relationship with amylin, it is of interest to establish the three-dimensional conformation of this polypeptide. Circular dichroism (CD) studies of CGRP have indicated a solvent-dependent tendency to adopt α-helical secondary structure (Lynch & Kaiser, 1988). Here, we report a nuclear magnetic resonance (NMR) study of the conformation of human CGRP (hCGRP) in 50% aqueous trifluoroethanol solution, in conjunction with distance geometry (DG), restrained energy minimization (REM), and restrained molecular dynamics (RMD) simulations.

Materials and Methods

Sample Preparation. Synthetic hCGRP-1 and hCGRP-2 (Bachem) were gifts from Celltech (Slough, U.K.) and Amylin Corp. (San Diego, CA). Perdeuterated trifluoroethanol (TFE-d_3; CEA, Gif-sur-Yvette, France) was used as supplied or after exchange of labile deuterons with protons (TFE-d_2). Peptide was dissolved to a final concentration of 10–18 mM in either 50% H_2O/50% TFE-d_2 or 50% D_2O/50% TFE-d_3. The pH was adjusted to a glass electrode reading of 3.7 (uncorrected for isotope effects).

NMR Spectroscopy. Proton NMR spectra of hCGRP were routinely recorded at 27 °C on Bruker AM series 500- or 600-MHz instruments, except for two HOHAHA experiments which were acquired on a home-built 500-MHz spectrometer comprising an Oxford Instruments magnet and a GE/Nicolet 1280 computer. Double-quantum-filtered 2-D correlation (DQF-COSY; Piantini et al., 1982; Rance et al., 1983) and exclusive correlation (E.COSY; Griesinger et al., 1985, 1987) spectra were acquired in the phase-sensitive mode by time-proportional phase incrementation of the first pulse (TPPI; Marion & Wüthrich, 1983). Phase-sensitive 2-D nuclear Overhauser effect (NOE) spectra (NOESY; Jeener et al., 1979; Kumar et al., 1981) were recorded with mixing times of 50, 200, and 400 ms using TPPI. Homonuclear Hartmann–Hahn (HOHAHA; Bax & Davis, 1985) spectra were acquired with mixing times of 28, 50, and 115 ms; phase-sensitive detection was achieved with TPPI (Bruker AM 600 spectrometer) or by the States method (States et al., 1982) on the home-built 500-MHz spectrometer. The solvent OH resonance was suppressed by irradiation during the relaxation delay (and, for NOESY, during the mixing time); in all except the HOHAHA experiments, a lower decoupler power was also applied throughout the t_1 period. The chemical shift reference was set at the center of the residual CDH resonance of deuteriotrifluoroethanol (3.88 ppm). Data were processed on Bruker Aspect 3000 or GE/Nicolet 1280 data stations, or on a Sun-4/110 computer using the FTNMR software package (Hare Research). NOE intensities, used as input for the distance geometry calculations, were determined from NOESY spectra at 50- and 200-ms mixing times by counting cross-peak contour levels and were classified into three distance ranges (0.2–0.25, 0.2–0.35, and 0.2–0.5 nm); 400-ms NOESY spectra were used only for assignment purposes.

Amide protons exhibiting perturbed rates of exchange with the solvent were identified at pH 3.7 following dissolution of protonated hCGRP-1 in 50% D_2O/50% TFE-d_3. Individual resonances were monitored over a period of 6 h in rapid (approximately 30 min) phase-sensitive COSY experiments.

Estimates of NH–CαH coupling constants ($^3J_{NH\alpha}$) were obtained from one-dimensional spectra (hCGRP-1 and hCGRP-2) or from an E.COSY spectrum acquired in protonated medium and with high digital resolution in F_2 (hCGRP-2). CαH–CβH coupling constants ($^3J_{\alpha\beta}$) for some residues of hCGRP-1 were recorded as passive couplings in slices taken parallel to F_2 from an E.COSY spectrum (maximum coherence order = 3) acquired in deuterated medium. These coupling constants were employed in conjunction with estimates of certain intraresidue NOE intensities in the stereospecific or rotamer assignment of the β-methylene protons of these residues. Similarly, stereospecific assignment of the γ-methyl groups of one valine residue (Val-8) was achieved by measurement of $^3J_{\alpha\beta}$ as an active coupling in the F_2 dimension of the same E.COSY spectrum, together with estimates of intraresidue NOE intensities.

Structure Calculations. Analysis of the NMR data produced 353 distance restraints, classified into distances as described previously. χ^1 dihedral angle restraints for certain residues based on rotamer classifications about the Cα–Cβ bond were also obtained (see Table II). The allowed ranges of these angles were ±60°. For residues Leu-15 and Leu-16, for which the E.COSY cross-peaks could be fitted to either the g^2t^3 or t^2g^3 rotamers and which could not be further distinguished from the NOESY data, χ^1 was constrained in the combined ranges, i.e., 180° ± 60° and −60° ± 60°. These data were used to generate structures using the program DISMAN (Braun & Go, 1985). A total of 50 structures were generated in this manner, and the best 24, based on an arbitrary final error function cutoff, were subsequently refined by REM and RMD using the GROMOS suite of programs (van Gunsteren & Berendsen, 1987).

Each of the structures to be refined was first subjected to 100 steps of steepest descents REM. The RMD simulations were performed as follows. Structures were equilibrated for 2 ps coupled to a temperature bath at 600 K with a T_c of 0.01 ps (Berendsen et al., 1984). The time step used throughout the simulations was 2 fs, and bond lengths were kept rigid by using the SHAKE algorithm (van Gunsteren & Berendsen, 1977). The force constant for the NOE distance restraints (K_{dc}) at this stage was 4000 kJ mol^{-1} nm^{-2}, and the force constant for the dihedral (K_{dh}) was 50.0 kJ mol^{-1}. RMD was then performed for 5 ps at 600 K (T_c = 0.1 ps) using a K_{dc} of 8000 kJ mol^{-1} nm^{-2} and a K_{dh} of 50.0 kJ mol^{-1}. This was followed by 10-ps cooling to 300 K (T_c = 2.0 ps) and 5-ps RMD at 300 K (T_c = 0.1 ps) with a K_{dc} of 1000 kJ mol^{-1} nm^{-2}. These last 5 ps, with a configuration saved every 0.1 ps, were used for analysis of time-averaged properties. The last 2 ps were averaged, and the resulting structures were energy-minimized (K_{dc} = 1000 kJ mol^{-1} nm^{-2}, K_{dh} = 7.0 kJ mol^{-1}) to provide "final" structures for conformational analysis. All

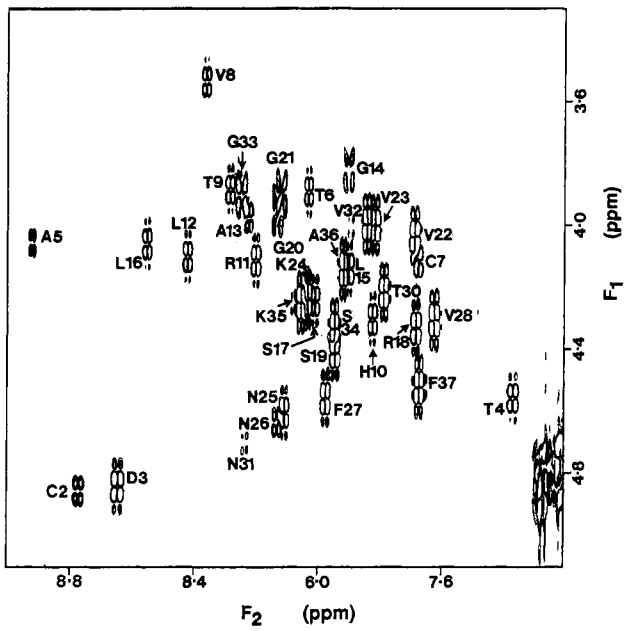

FIGURE 1: Region of the 600-MHz DQF-COSY spectrum of hCGRP-1 recorded in 50% TFE/50% H_2O, pH 3.7, 27 °C, showing NH–CαH cross-peaks labeled according to residue.

computational procedures were performed on Sun-4 series computers.

Results

Sequential Assignment and Secondary Structure Elements. Initial NOESY spectra of hCGRP-1 or hCGRP-2 recorded at pH 3.7 in 90% H_2O/10% D_2O (the latter was present to provide a lock signal) were devoid of all but a few intraresidue and sequential (i–i+1) NOEs, indicating rapid conformational fluctuation and/or a lack of well-defined three-dimensional structure under these conditions. Because CD analysis of hCGRP had indicated that addition of trifluoroethanol increases the apparent helical content of the molecule (Lynch & Kaiser, 1988), subsequent experiments were conducted in 50% H_2O (or D_2O)/50% TFE.

At pH 3.7 and 27 °C in H_2O/TFE-d_2, it was possible to identify 35 out of 36 theoretically observable amide proton resonances in the NH–CαH ("fingerprint") cross-peak region of DQF-COSY spectra of hCGRP-1 (Figure 1) or hCGRP-2. Virtually complete assignment of resonances in both hCGRPs was achieved by the sequential assignment procedure of Wüthrich et al. (1982); chemical shifts for hCGRP-1 are presented in Table I. Briefly, the technique entails establishing the identity of amino acid spin systems from DQF-COSY (which manifests connectivities between protons separated by up to three bonds), HOHAHA (giving remote connectivities), and NOESY spectra; individual spin systems are placed in the amino acid sequence by identification of characteristic ("sequential") interresidue NOEs (typically, NH_i–NH_{i+1}, $C\alpha H_i$–NH_{i+1}, and $C\beta H_i$–NH_{i+1}). Only the meta and para ring protons of Phe-27, and all the ring protons of Phe-37, evaded assignment owing to near-degeneracy of resonances and a lack of NOEs to these protons (the latter presumably due to relatively high local mobility of the C-terminal residue; see later). It is notable that all spectra were very similar for both hCGRP-1 and hCGRP-2; indeed, the only major resonance shifts were associated with protons assigned to the three substituted amino acid residues themselves.

The type and relative intensity of sequential and longer range NOEs observed in a given region of the sequence can yield clues to the prevailing secondary structure; these are summarized for hCGRP-1 in Figure 2. Figure 3 shows the NH–NH region of the 200-ms NOESY spectrum of hCGRP-2. A preponderance of strong NH_i–NH_{i+1} NOEs (together with relatively weak $C\alpha H_i$–NH_{i+1} NOEs) in the sequence between Thr-6 and Arg-18 was suggestive of helical structure in this region. This inference was further supported by the observation of NOEs between the Cα proton of residue i and the amide proton of residue i+3 for most of the residues between Ala-5 and Ser-17 (Figure 2). Also characteristic of α-helical structure were a number of $C\alpha H_i$–$C\beta H_{i+3}$ and $C\alpha H_i$–NH_{i+4} NOEs in this region of the sequence. Consistent with these NOE patterns were the apparent NH–CαH coupling constants measured from 1-D spectra of both hCGRPs and from E.COSY spectra of hCGRP-2, which for residues Thr-6 to Ser-17 (excluding Gly-14) were all within the range 4.4–5.8 Hz (Figure 4); these are close to the "classical" α-helix value of 3.9 Hz. Furthermore, the amide protons of Thr-9,

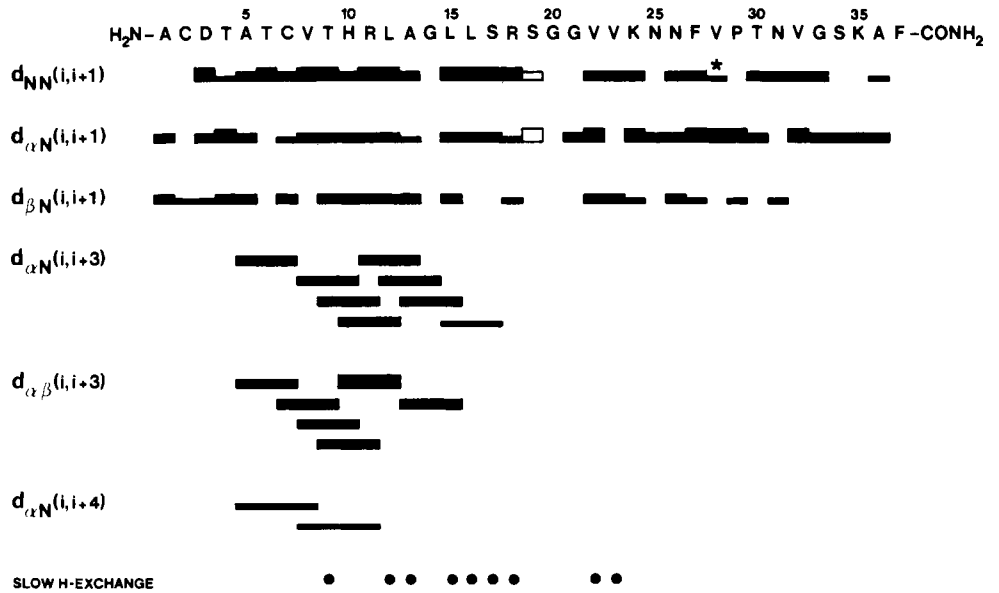

FIGURE 2: Diagrammatic representation of sequential and secondary structural interresidue NOEs observed for hCGRP-1 in 50% TFE/50% H_2O, pH 3.7, 27 °C. NOE intensities are indicated by the heights of the bars. Unfilled bars indicate uncertainty in assignment of NOEs involving the amide protons of Gly-20 or Gly-21, whose resonances were almost coincident; the asterisk denotes NOEs to the CδH protons of Pro-29. Also shown are residues for which slow exchange of NH protons with deuterons was observed.

Table I: Proton Chemical Shifts of hCGRP-1[a]

residue	chemical shift (ppm) NH	αH	βH	others	residue	chemical shift (ppm) NH	αH	βH	others
Ala-1		4.00	βCH_3 1.47		Val-22				0.93
Cys-2	8.77	4.84	3.02		Val-23	7.81	4.00	2.04	γCH_3 0.88
			3.11						0.88
Asp-3	8.64	4.83	2.70		Lys-24	8.03	4.24	1.72	γCH 1.38
			2.88					1.79	1.38
Thr-4	7.36	4.55	4.57	γCH_3 1.32					δCH 1.63
Ala-5	8.92	4.05	βCH_3 1.44						1.65
Thr-6	8.03	3.89	4.00	γCH_3 1.13					εCH 2.94
Cys-7	7.68	4.12	3.19						2.94
			3.35						ζNH_3^+ 7.50
Val-8	8.36	3.53	2.05	γCH_3 0.90	Asn-25	8.10	4.60	2.67	δNH 7.39
				0.98				2.73	6.63
Thr-9	8.28	3.88	4.15	γCH_3 1.24	Asn-26	8.13	4.63	2.61	δNH 7.30
His-10	7.83	4.30	3.28	2H 8.49				2.67	6.61
			3.34	4H 7.28	Phe-27	7.97	4.55	3.01	2,6H 7.18
Arg-11	8.19	4.11	1.96	γCH 1.65				3.07	3,5H NR
			2.06	1.84					4H NR
				δCH 3.18	Val-28	7.62	4.30	1.98	γCH_3 0.85
				3.18					0.88
				εNH 7.12	Pro-29		4.36	1.94	γCH 1.99
Leu-12	8.41	4.09	1.62	γCH 1.70				2.22	1.99
			1.74	δCH_3 0.81					δCH 3.55
				0.83					3.66
Ala-13	8.21	3.97	βCH_3 1.41		Thr-30	7.78	4.21	4.19	γCH_3 1.17
Gly-14	7.90	3.77			Asn-31	8.23	4.69	2.76	δNH 7.42
		3.84						2.82	6.66
Leu-15	7.90	4.13	1.65	γCH 1.68	Val-32	7.84	4.00	2.08	γCH_3 0.88
			1.84	δCH_3 0.86					0.90
				0.86	Gly-33	8.24	3.86		
Leu-16	8.55	4.05	1.44	γCH 1.74			3.93		
			1.79	δCH_3 0.78	Ser-34	7.94	4.33	3.82	
				0.78				3.91	
Ser-17	8.01	4.24	3.97		Lys-35	8.05	4.24	1.72	γCH 1.38
			4.01					1.79	1.38
Arg-18	7.69	4.32	1.87	γCH 1.69					δCH 1.63
			1.96	1.76					1.65
				δCH 3.15					εCH 2.94
				3.15					2.94
				εNH 7.14					ζNH_3^+ 7.50
Ser-19	7.94	4.41	3.92		Ala-36	7.91	4.14	βCH_3 1.18	
			3.97		Phe-37	7.67	4.52	2.96	2,6H NR
Gly-20	8.12	3.90						3.15	3,5H NR
		3.98							4H NR
Gly-21	8.11	3.85							CONH 6.85
		3.93							7.19
Val-22	7.69	4.03	2.06	γCH_3 0.89					

[a] Assignments were obtained in 50% TFE/50% H_2O (or D_2O) at 27 °C and pH 3.7, and are quoted relative to the residual CDH resonance of TFE-d_2 or TFE-d_3 (3.88 ppm). NR indicates resonance not resolved under these conditions.

Leu-12, Ala-13, Leu-15, Leu-16, and Ser-17 in hCGRP-1 were relatively slow to exchange with solvent deuterons (Figure 2), consistent with participation in hydrogen bonds.

NOEs observed between residues in the N-terminal region of hCGRP reflected the influence of the disulfide bond between Cys-2 and Cys-7. A comparatively well-defined loop structure was indicated by NOEs between Cys-2 CαH and both Cys-7 Cβ protons, and from both Cys-2 Cβ protons to the *pro*-S γ-methyl protons of Val-8; indeed, NOEs to Val-8 γ-methyl protons from protons in residues Asp/Asn-3, Thr-4, Ala-5, Thr-6, and Cys-7 were observed. $^3J_{NH\alpha}$ coupling constants (measured as apparent splittings in an E.COSY spectrum of hCGRP-2) assumed moderately large values for Asn-3 (9.1 Hz) and Thr-4 (8.0 Hz), and a very small value for Ala-5 (<3.0 Hz), indicating that this region of the sequence has a relatively constrained conformation enforced upon it by the disulfide bond.

While the helical region (as defined by the NOE, coupling constant, and hydrogen bond information) clearly terminates in the region of Arg-18, it proved rather more difficult to establish with confidence the main-chain conformation in the region immediately following this residue. Certain features suggestive of a turn configuration were observed (for example, slow exchange of the amide proton of Arg-18 of hCGRP-1); however, unequivocal identification by NMR of distances characteristic of the "classical" turn types [e.g., $d_{\alpha N}(i+1,i+2)$, $d_{\alpha N}(i+1,i+3)$, and $d_{NN}(i+2,i+3)$ for type II β-turn; $d_{NN}(i+1,i+2)$ and $d_{\alpha N}(i+2,i+3)$ for type I β-turn] depends critically upon resolution of the NH proton chemical shifts of residues $i+2$ and $i+3$. In the case of both hCGRP-1 and hCGRP-2, a strong NOE interaction was indeed observed between the Cα proton of Ser-19 and the NH proton of either Gly-20 or Gly-21, but the virtual coincidence of the amide proton shifts of these latter residues hampered discrimination between possible turn types. Also precluded was the observation of any NH_{i+2}–NH_{i+3} NOE interaction which, again, would be anticipated for any of the standard turn types. A NOESY spectrum of hCGRP-1 acquired at 12 °C failed to alleviate the chemical shift overlap.

In contrast to the relatively well-defined secondary structure of the amino-terminal half of the molecule, the region between Val-22 in hCGRP-1 (Met-22 in hCGRP-2) and the C-ter-

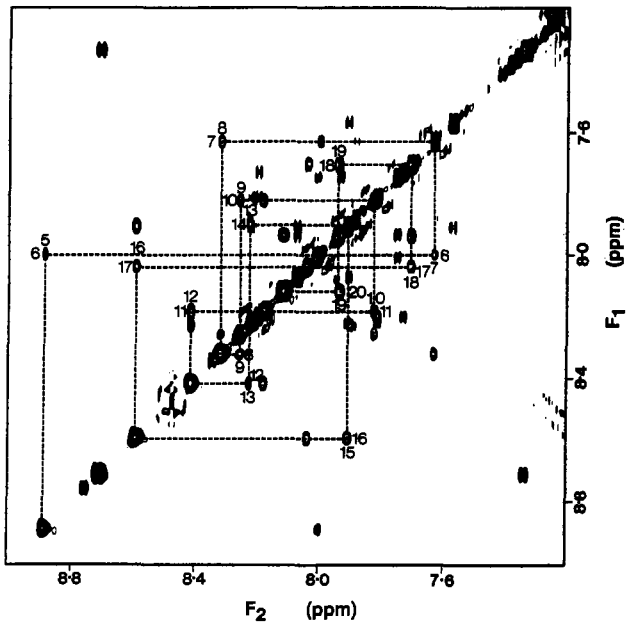

FIGURE 3: Region of the 500-MHz NOESY spectrum of hCGRP-2 showing sequential NH–NH connectivities in the region from Ala-5 to Gly-20 labeled according to residue. The spectrum was recorded with a mixing time of 200 ms in 50% TFE/50% H_2O, pH 3.7, 27 °C.

minus at Phe-37 was characterized by close-to-random-coil resonance shifts, the presence of $C\alpha H_i$–NH_{i+1} and NH_i–NH_{i+1} NOEs of similar intensity, and a complete lack of identifiable medium-range interactions. Experimentally determined $^3J_{NH\alpha}$ coupling constants for this region of the polypeptide chain were all in the range 5.9–7.9 Hz (Figure 4), typical of "random coil" or dynamically averaged ϕ dihedral angles. Nor (with the exception of Val-22 and Val-23) were rates of exchange of amide protons with solvent deuterons noticeably perturbed over most of this region in hCGRP-1, consistent with a lack of any stable, hydrogen-bonded structure (Figure 2). Collectively, these observations constitute evidence for a predominantly disordered structure over this stretch of the polypeptide chain. Interestingly, any conformational heterogeneity in the region of Pro-29 was not manifested in the observed NOEs; the presence of NOEs betwen the NH proton of Val-28 and the CδH protons of Pro-29 in the absence of CαH–CαH NOEs for these residues indicates the exclusive adoption of the trans peptide bond conformation by Pro-29.

While certain secondary structure elements could be identified from the NOE data as described above, there was no evidence for the existence of a well-defined tertiary fold in hCGRP; no NOEs were observed between residues more than five removed in the sequence, implying an absence of stable close contacts between the N-terminal loop and helix region and the poorly defined carboxy-terminal tail in solution.

Stereospecific assignments of prochiral β-methylene protons and of isopropyl groups of valine residues can lead to better definition of the backbone fold in addition to establishing the χ^1 dihedral angle where there is one predominant side-chain rotamer (Hyberts et al., 1987; Driscoll et al., 1989). For hCGRP-1, cross-peak overlap or values of $^3J_{\alpha\beta}$ coupling constants or intraresidue NOE intensities indicative of motional averaging of the side chain precluded rotamer assignment in most cases. However, unequivocal stereospecific or rotamer assignments, or excluded values of χ^1, could be obtained for a few residues in the N-terminal loop and helix regions; these are summarized in Table II.

Structure of hCGRP by Distance Geometry and Molecular Dynamics. Following DISMAN, 24 structures were subjected

Table II: Side-Chain Rotamer Assignments for hCGRP-1[a]

(i) β-Methylene Groups

residue	$J_{\alpha\beta}$H	$J_{\alpha\beta}$L	$d_{\alpha\beta}$H	$d_{\alpha\beta}$L	$d_{NH\beta}$H	$d_{NH\beta}$L	rotamer (±60°)
Asp-3	4.1	5.9	S	S	W/M	M	+60°
Leu-15	6.1	9.2	NR	NR	M	M	*not* +60°
Leu-16	4.1	10.8*	NR	NR	W/M	NR	*not* +60°
Ser-17	5.0	4.1	S	S	NR	NR	+60°
Ser-19	5.1	5.2	S	S	NR	NR	+60°

(ii) γ-Methyl Groups

residue	$J_{\alpha\beta}$	$d_{\alpha\beta}$	$d_{NH\beta}$	$d_{\alpha\gamma}$H	$d_{\alpha\gamma}$L	$d_{NH\gamma}$H	$d_{NH\gamma}$L	rotamer (±60°)
Val-8	10.2	M/S	S	S	S	W	S	180°

[a] The table lists residues in hCGRP-1 for which it was possible either to obtain unequivocal side-chain rotamer assignments or to exclude one of the preferred rotamers. $^3J_{\alpha\beta}$ coupling constants (in hertz) for residues containing β-methylene groups were measured as passive displacements (except for asterisk, active coupling) from an E.COSY spectrum of hCGRP-1 recorded in deuterated medium; the value of $^3J_{\alpha\beta}$ for Val-8 was determined as the active coupling from the same spectrum. Estimates of intraresidue NOE intensities were obtained from phase-sensitive NOESY spectra recorded in protonated medium with mixing times of 50 and 200 ms, and were classified into five distance ranges (weak, weak/medium, medium, medium/strong, and strong); NR indicates cross-peak insufficiently resolved to provide a reliable estimate of NOE intensity. Suffixes H and L indicate high-field and low-field members of pairs of methylene protons or γ-methyl groups, respectively. The assignment of the side-chain to the preferred rotamer (±60°) most closely corresponding to the data is indicated. All other side chains for which $^3J_{\alpha\beta}$ coupling constants could be determined yielded values incompatible with a single preferred rotamer.

to refinement by RMD, yielding a mean sum-of-restraint-violations of 2.06 ± 0.18 nm and a mean potential energy of −2017 ± 132 kJ mol^{-1}. The convergence achieved over the well-defined region was also good: the rms deviation for the backbone atoms of residues 2–18 is 1.08 Å, while for all atoms it is 1.99 Å.

The distribution of backbone dihedral angles in these structures (Figure 4A,B) reflects the extent to which conformation has been defined by NOE restraints. The disulfide-bridged loop (residues 2–7 inclusive) apparently falls into either of two closely similar minimum energy conformations upon minimization, but discrimination between the two on the basis of best fit to the NMR data is not possible. Good agreement was observed between the experimentally determined and calculated values of ϕ for the helical region (Val-8 to Leu-16). In contrast, the lack of convergence to a consensus structure from residue Ser-19 onward reflects the absence of structurally significant NOE data for this region of the polypeptide. Although the NOE restraints for this region are clearly time-averaged values, they are exclusively of the i–i+1 type, and hence their use in conventional static-bounds DISMAN/RMD simulations has not unacceptably prejudiced the searching of conformational space, as might have occurred had longer range NOEs been observed (Torda et al., 1990).

Calculated hydrogen bond occupancies for residues Leu-12, Ala-13, Leu-15, and Leu-16 from the RMD trajectories are all in excess of 90% and show the expected NH_i–CO_{i-4} pattern, in agreement with the observation of slowly exchanging NH resonances for these residues. However, similar analyses for residues Thr-9, Ser-17, Val-22, and Val-23 show no correlation with hydrogen bonds characteristic of any regular secondary structure. Thr-9 shows no long-lived hydrogen bonds during the simulations, while Ser-17 shows an α-helical (NH_i–CO_{i-4}) hydrogen bond to Ala-13 for approximately 40% of the time. Val-22 and Val-23 show NH_i–CO_{i-3}-type hydrogen bonds present for only ca. 30% of the time. Thus, the structures

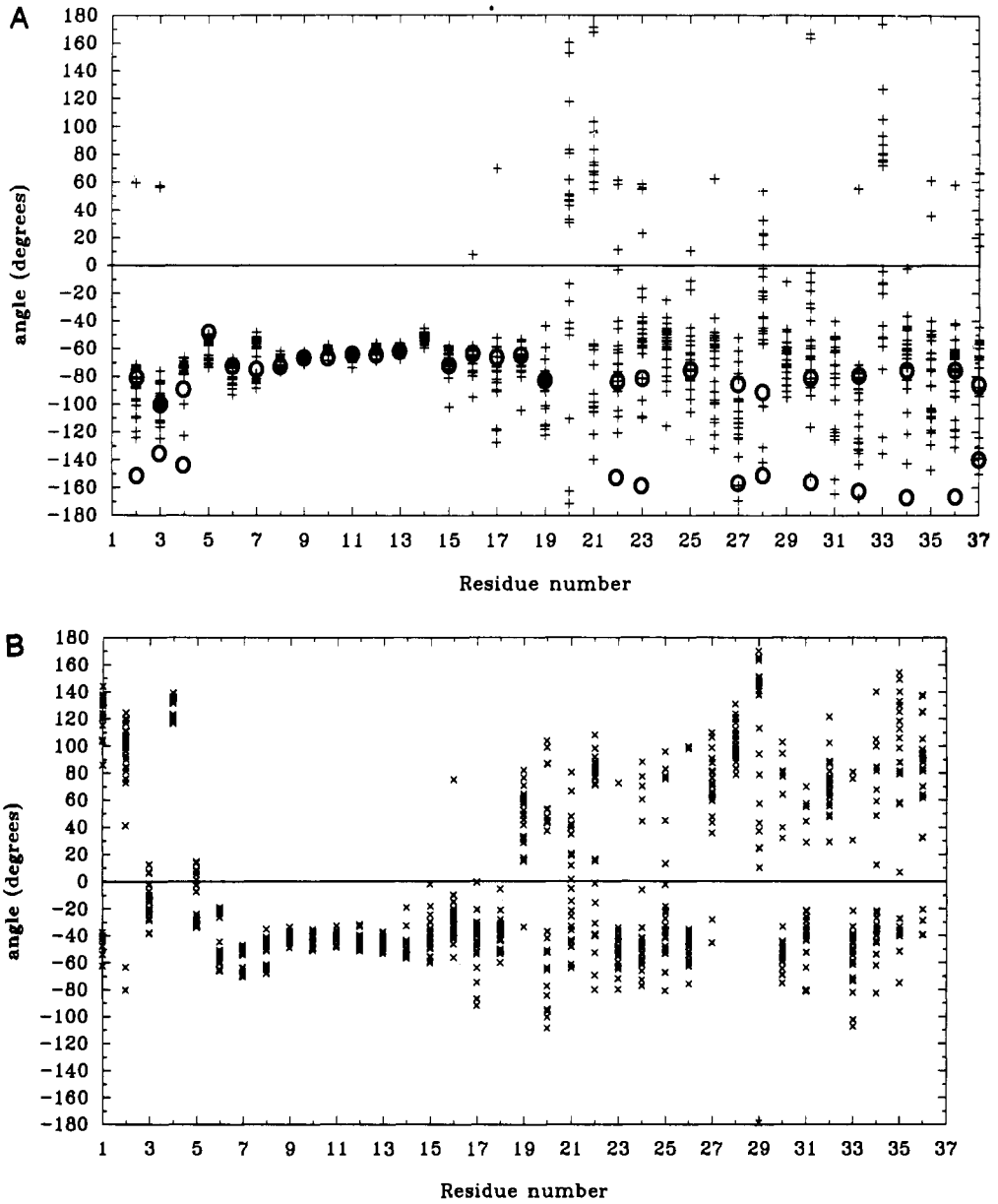

FIGURE 4: (A) Comparison of backbone ϕ dihedral angle as a function of residue number derived experimentally (O) or from the 24 final dynamics structures (+) for hCGRP-1. Apparent $^3J_{NH\alpha}$ coupling constants were obtained from 1-D spectra or E.COSY spectra recorded with high digital resolution in the acquisition dimension and are not corrected for line-width contributions (NH line width was typically 3.5–4.5 Hz). ϕ dihedral angles were calculated according to the equation given by Pardi et al. (1984). Where experimentally determined coupling constants are consistent with more than one ϕ dihedral angle, both are indicated except in regions of the sequence for which NOE information predicted helical structure. (B) ψ angles calculated from the final structures plotted versus residue number.

calculated do not completely explain the observed pattern of slowly exchanging amides in hCGRP-1 (Figure 2).

Figure 5A shows a superposition of all 24 structures (only the well-defined region covering residues Cys-2 to Arg-18 is shown for clarity). The apparent lack of convergence in the N-terminal loop results primarily from variability in its relative position with respect to the helical section. Figure 5B shows the loop overlaid over the backbone atoms of residues 2–7 only. The two alternative conformations of the disulfide bridge can be seen.

Discussion

We have been able to achieve virtually complete assignment of the ^{1}H NMR spectrum of hCGRP-1 in a 1:1 TFE/water solution; moreover, the spectrum of hCGRP-2 was sufficiently similar to be assignable by comparison with that of the former analogue, without recourse to de novo sequential assignment. Regions of defined secondary structure could be identified readily from the observed NOE patterns, although a substantial portion of the sequence was apparently devoid of regular structure according to this criterion. These inferences were corroborated by experimental amide-α proton coupling constants and by amide proton exchange information. NOEs identified from 50- amd 200-ms NOESY spectra of hCGRP-1 were classified according to intensity and employed as distance restraints for structure calculations by using the distance geometry program DISMAN and subsequent refinement with the molecular simulation package GROMOS.

Our structure for hCGRP in this solvent consists of a well-defined N-terminal loop followed by approximately three turns of α-helix; this ends in a poorly defined turn leading into the C-terminal region which is predominantly unconstrained by the NMR data and, by implication, lacks significant stable structure. In contrast, our initial characterization of hCGRP in aqueous medium indicated that the molecule is devoid of *any* regular secondary structure under these conditions, con-

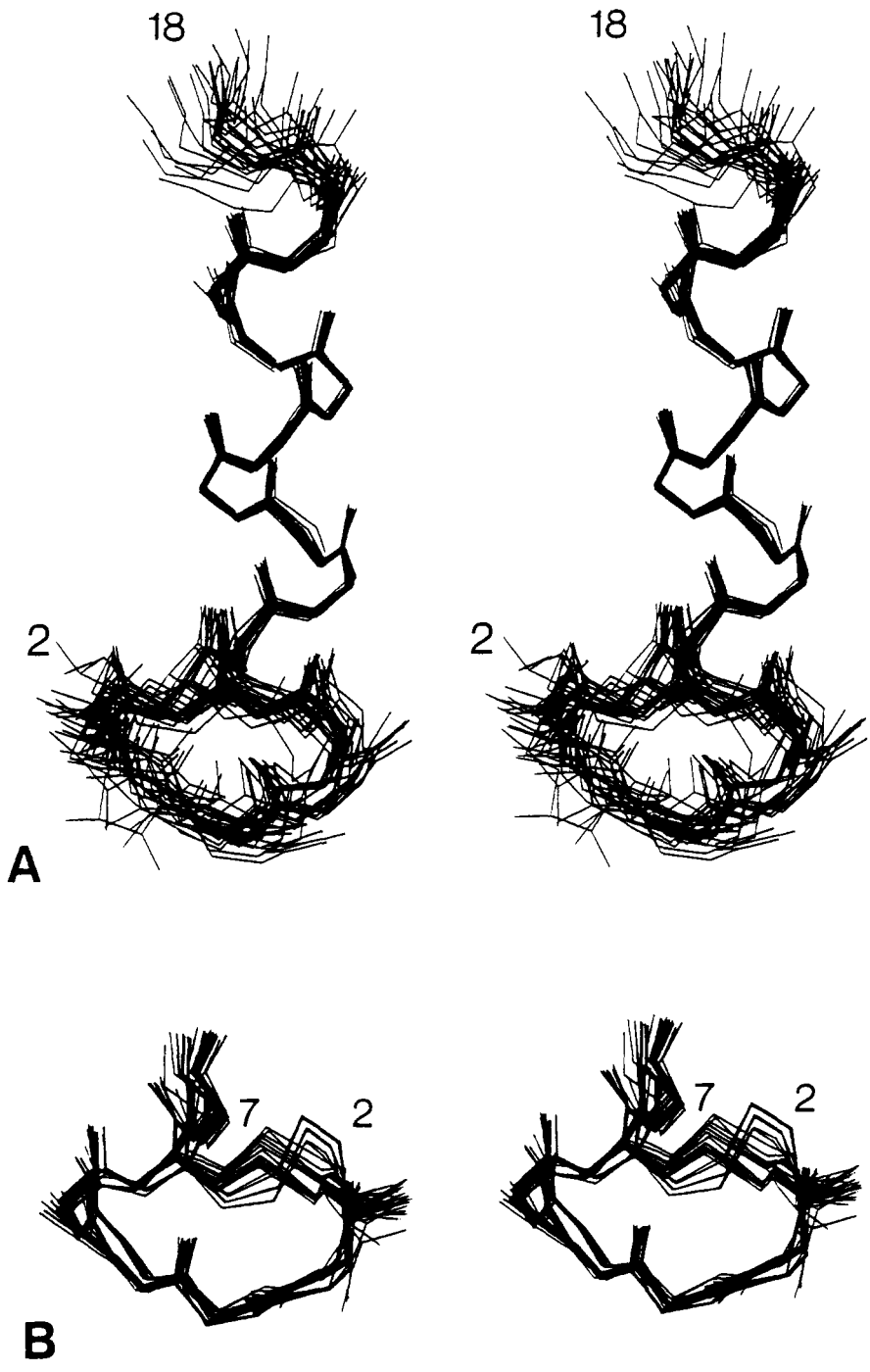

FIGURE 5: (A) Stereoview of the 24 final structures of hCGRP-1 overlaid over the backbone atoms of residues 2–18 (this well-defined region only is shown for clarity). (B) shows the disulfide-bridged loop (residues Cys-2 to Cys-7) overlaid over the Cα atoms of these residues, demonstrating the divergence of the structures in this region.

sistent with CD studies which have indicated a significant increase in the α-helical content of rat CGRP in buffer containing 50% TFE over that detected in purely aqueous medium (Lynch & Kaiser, 1988). This is a characteristic which CGRP evidently shares with a number of other peptide hormones predicted to form amphiphilic α-helices (Kaiser & Kezdy, 1984). The influence of lipid micelles or organic solvents such as TFE on the experimentally determined secondary structure of such hormones is commonly held to be consistent with a role for the membrane lipid–water interface in stabilizing an active conformation at the receptor. Our identification of a 10-residue α-helical region displaying an amphiphilic distribution of hydrophobic and hydrophilic amino acids lends further credence to this mechanism for CGRP; furthermore, the localization of stable α-helix to a discrete region of the molecule demonstrates that the induction of secondary structure by TFE/water mixtures is not indiscriminate and vindicates the use of this solvent for such studies.

Existing information concerning the relationship between structure and activity for CGRP largely hinges upon the effects of residue deletions/substitutions and of chemical modifications on biological activity. All tryptic fragments of CGRP are inactive, indicating that essentially the intact sequence is required (Breimer et al., 1988). Furthermore, both N- and C-terminal regions seem to be important for agonist activity: linearization of the N-terminal disulfide-bonded loop region by reduction and S-carboxamidomethylation abolishes activity, while acetylation of the N-terminus or of either lysine residue results in a marked reduction in potency (Breimer et al., 1988). Conversely, the synthetic fragment hCGRP-(8–37) has re-

cently been demonstrated to be a specific antagonist for CGRP receptors in rat liver plasma membranes (Chiba et al., 1898). Hence, it appears that the amphiphilic α-helix identified here is likely to play a major role in the interaction of the molecule with its receptor, while the N-terminal loop region may principally be involved in triggering the ensuing signal-transduction process.

CGRP causes insulin resistance in skeletal muscle in vitro, a property it shares with amylin, the monomer component of the type 2 diabetic pancreas amyloid (Leighton & Cooper, 1988). There exists 46% overall sequence homology between amylin and hCGRP-2, with particularly high agreement in the N- and C-terminal regions (Cooper et al., 1987). Since both polypeptides are of the same length (37 residues) and possess a disulfide bond between cysteines-2 and -7 (Cooper et al., 1987), it is probable that at least some of the secondary structural characteristics identified here for CGRP (particularly in the N-terminal loop and helix regions) are shared by amylin. Although a weaker homology to the A chain of insulin was identified (Cooper et al., 1987), comparison of our structure for CGRP with the X-ray crystal structure of porcine insulin showed both the geometry of the polypeptide backbone and the disposition of the side chains, particularly in the disulfide-bonded loop regions where the highest degree of homology was detected, to be quite different in the two molecules. It therefore seems unlikely that the sequence homology is of any functional significance.

ACKNOWLEDGMENTS

We thank Garth Cooper of Amylin Corp. for introducing us to this molecule and Dennis Hare, Werner Braun, and Wilfred van Gunsteren for the gifts of the FTNMR, DISMAN, and GROMOS programs, respectively.

Registry No. CGRP, 90954-53-3.

REFERENCES

Amara, S. G., Jonas, V., Rosenfeld, M. G., Ong, E. S., & Evans, R. M. (1982) *Nature (London) 289*, 240–245.

Bax, A., & Davis, D. G. (1985) *J. Magn. Reson. 65*, 355–360.

Berendsen, H. J. C., Postma, J. P. M., van Gunsteren, W. F., Di Nola, A., & Haak, J. M. (1984) *Proc. Natl. Acad. Sci. U.S.A. 81*, 3684–3690.

Braun, W., & Go, N. (1985) *J. Mol. Biol. 186*, 611–626.

Breimer, L. H., MacIntyre, I., & Zaidi, M. (1988) *Biochem. J. 255*, 377–390.

Chiba, T., Yamaguchi, A., Yamatani, T., Nakamura, A., Morishita, T., Inui, T., Fukase, M., Noda, T., & Fujita, T. (1989) *Am. J. Physiol. 256*, E331–E335.

Cooper, G. J. S., Willis, A. C., Clark, A., Turner, R. C., Sim, R. B., & Reid, K. B. M. (1987) *Proc. Natl. Acad. Sci. U.S.A. 84*, 8628–8632.

Cooper, G. J. S., Leighton, B., Dimitriadis, G. D., Parry-Billings, M., Kowalchuk, J. M., Howland, K., Rothbard, J. B., Willis, A. C., & Reid, K. B. M. (1988) *Proc. Natl. Acad. Sci. U.S.A. 85*, 7763–7766.

Driscoll, P. C., Gronenborn, A.M., & Clore, G. M. (1989) *FEBS Lett. 243*, 223–233.

Fisher, D. A., Kikkawa, D. O., Rivier, J. E., Amara, S. G., Evans, R. M., & Rosenfeld, M. G. (1983) *Nature (London) 305*, 534–536.

Gibson, S. J., Polak, J. M., Bloom, S. R., Sabate, I. M., Mulderry, P. K., Ghatei, M. A., McGregor, J. P., Morrison, J. F. B., Kelly, J. S., Evans, R. M., & Rosenfeld, M. G. (1984) *J. Neurosci. 4*, 1301–1311.

Griesinger, C., Sørensen, O. W., & Ernst, R. R. (1985) *J. Am. Chem. Soc. 107*, 6394.

Griesinger, C., Sørensen, O. W., & Ernst, R. R. (1987) *J. Magn. Reson. 75*, 474–492.

Hoppener, J. W. M., Steenbergh, P. A., Zandberg, J., Geurts van Kessel, A. H. M., Baylin, S. B., Nelkin, B. D., Jansz, H. S., & Lips, C. J. M. (1985) *Hum. Genet. 70*, 259–263.

Hyberts, S. G., Märki, W., & Wagner, G. (1987) *Eur. J. Biochem. 164*, 625–635.

Jeener, J., Meier, B. H., Bachmann, P., & Ernst, R. R. (1979) *J. Chem. Phys. 71*, 4546–4553.

Kaiser, E. T., & Kezdy, F. J. (1984) *Science 223*, 249–255.

Kimura, S., Sugita, Y., Kanazawa, I., Saito, A., & Goto, K. (1987) *Neuropeptides 9*, 75–82.

Kumar, A., Ernst, R. R., & Wüthrich, K. (1981) *Biochem. Biophys. Res. Commun. 95*, 1–6.

Leighton, B., & Copper, G. J. S. (1988) *Nature (London) 335*, 632–635.

Lynch, B., & Kaiser, E. T. (1988) *Biochemistry 27*, 7600–7607.

Marion, D., & Wüthrich, K. (1983) *Biochem. Biophys. Res. Commun. 113*, 967–974.

Morris, H. R., Panico, M., Etienne, T., Tippins, J., Girgis, S. I., & MacIntyre, I. (1984) *Nature (London) 308*, 746–748.

Pardi, A., Billeter, M., & Wüthrich, K. (1984) *J. Mol. Biol. 180*, 741–751.

Piantini, U., Sørensen, O. W., & Ernst, R. R. (1982) *J. Am. Chem. Soc. 104*, 6800–6801.

Rance, M., Sørensen, O. W., Bodenhausen, G., Wagner, G., Ernst, R. R., & Wüthrich, K. (1983) *Biochem. Biophys. Res. Commun. 117*, 479–485.

Rosenfeld, M. G., Mermod, J.-J., Amara, S. G., Swanson, L. W., Sawchenko, P. E., Rivier, J., Vale, W. W., & Evans, R. M. (1983) *Nature (London) 304*, 129–135.

States, D. J., Haberkorn, R. A., & Ruben, D. J. (1982) *J. Magn. Reson. 48*, 286–292.

Steenbergh, P. H., Hoppener, J. W. M., Zandberg, J., Lips, C. J. M., & Jansz, H. S. (1985) *FEBS Lett. 183*, 403–407.

Struthers, A. D., Brown, M. J., Beacham, J. L., Morris, H. R., & MacIntyre, I. (1986) *J. Endocrinol. 107s*, 129.

Torda, A. E., Scheek, R. M., & van Gunsteren, W. F. (1990) *J. Mol. Biol. 214*, 223–235.

van Gunsteren, W. F., & Berendsen, H. J. C. (1977) *Mol. Phys. 34*, 1311–1327.

van Gunsteren, W. F., & Berendsen, H. J. C. (1987) *GROMOS Manual*, Biomos, Groningen.

Westermark, P., Wernstedt, C., Wilander, E., Hayden, D. W., O'Brien, T. D., & Johnson, K. H. (1987) *Proc. Natl. Acad. Sci. U.S.A. 84*, 3881–3885

Wüthrich, K., Wider, G., Wagner, G., & Braun, W. (1982) *J. Mol. Biol. 155*, 311–319.